

# Adsorption Kinetics of Acid Red on Activated Carbon Web Prepared from Acrylic Fibrous Waste

M. Salman Naeem<sup>1\*</sup>, Saima Javed<sup>2</sup>, Vijay Baheti<sup>1</sup>, Jakub Wiener<sup>1</sup>, M. Usman Javed<sup>1</sup>,  
Syed Zameer Ul Hassan<sup>3</sup>, Adnan Mazari<sup>1</sup>, and Jawad Naeem<sup>1</sup>

<sup>1</sup>Faculty of Textile Engineering, Department of Material Engineering, Technical University of Liberec, Liberec 46117, Czech Republic

<sup>2</sup>Department of Microbiology and Molecular Genetics, Punjab University, Lahore, Punjab 54590, Pakistan

<sup>3</sup>Department of Textile Engineering, Balochistan University of Information Technology, Engineering and Management Sciences, Quetta 87650, Pakistan

(Received February 25, 2017; Revised October 29, 2017; Accepted November 2, 2017)

**Abstract:** In this work, activated carbon (AC) web was prepared using physical activation under the layer of charcoal in high temperature furnace. The carbonization of acrylic fibrous waste was performed at different temperatures (800 °C, 1000 °C, and 1200 °C) with heating rate of 300 °C/h and at different holding time. At 1200 °C, the heating rate of 300 °C/h and no holding time provided better results of surface area as compared to carbonization at 800 °C and 1000 °C. The activated carbon web (AC) prepared at 1200 °C was used for removal of Acid Red 27 dye from aqueous media by varying different parameters like initial concentration of dye, stirring speed, adsorbent dosage, and pH. The results were evaluated using non-linear forms of Langmuir and Freundlich isotherms. The Freundlich isotherm was found to describe the results more effectively because of non-homogenous surface of activated carbon web. Further, the kinetics of adsorption was examined using linear and non-linear forms of pseudo 1st order and pseudo 2nd order.

**Keywords:** Physical activation, Stabilization, Carbonization, Heating rate, Holding time, Activated carbon

## Introduction

Rapid industrialization due to development in the field of science and technology with huge burden of population is causing a severe threat to environment. One of the most important sources of pollution is excessive use of dyes these days. The use of dyes is increasing day by day due to increased demand in leather, tanning, paper production, and textile industries. Dyes are used to give colors and currently more than 10,000 dyes with a production of 1 million tons under different trade names are used [1]. Acid red 27 is anionic dye used to color synthetic and natural fibers. Although this dye has been banned in many countries due to suspected carcinogenic, it is still used in many countries. The use of synthetic dyes is increasing due to their low cost, but their complex structure makes them difficult to degrade causing more difficulty in their removal from waste water effluent [2,3]. Different waste water techniques are being used for removal of wastes like biological, chemical, and physical methods. As synthetic dyes have complex aromatic structure, they are not removed by biological methods due to their low bio-degradation behavior [4]. Chemical techniques are not only expensive, but also result in accumulation of sludge which in turn creates problem of disposal [2]. Physical adsorption is very effective method for the removal of dyes from waste water. In physical adsorption, activated carbon (AC) is widely used as adsorbent material. Around 80 % of produced activated carbon is used in liquid phase

applications. The additional benefits of adsorption are cost effective, simple, and devoid of hazardous material [5-8].

Mainly physical and chemical methods are employed for the formation activated carbon. Chemical methods use the impregnation of precursor material with different chemicals like NaOH, KOH, ZnCl<sub>2</sub>, etc. followed by heating in inert atmosphere using temperature range of 450-900 °C. However, in physical activation after carbonizing material at high temperature the material is exposed with oxidizing gases in temperature range around 1000-1200 °C. Different precursors that are already in use for the formation of activated carbon are categorized as polyimides, polyacrylamides, phenolic resins [9,10], PAN, and cellulose based fibers [11]. Nowadays focus has been shifted towards the use of waste materials for effective utilization in order to keep environment more safe and protective. The statistics showed that generation of textile and clothing waste in UK is of the order of 2 million tons per year. This means 33 kg of clothing and textile waste per person in UK with a population of 500 million for the 27 countries of European Union equates to approximately 16.5 million tons. Textile waste is mainly categorized in two ways, natural fibers (cotton, wool, flax, etc.) and synthetic fibers (polyester, acrylic, nylon, etc.) [12]. In this context, the idea of using acrylic fibrous waste for the formation of activated carbon is attractive, as cost of activated carbon can be reduced along with effective utilization of textile waste. Further, the additional benefits of using acrylic fibrous wastes are possible high yield, better purity, high density, and dust free nature of activated carbon [13].

In this work, acrylic fibrous waste after converting into

\*Corresponding author: muhammad.salman.naeem@tul.cz

non-woven web was carbonized to activated carbon web by physical activation in high temperature furnace. Later, the yield %, specific surface area, shrinkage, flexibility, and dusting tendency of carbonized samples were determined. The study presented the utility of prepared activated carbon web for the removal of acid red 27 dyes from aqueous solution using adsorption kinetics.

## Experimental

### Materials

The acrylic fibrous waste was taken from Grund Industries of Czech Republic in the form of bath mats. These fibers have acrylonitrile copolymer 85-89 %. The physical characteristics of acrylic fibers are shown in Table 1.

Acid red 27 was purchased from Sigma Aldrich, Czech Republic. The structure and properties of acid red are given in Table 2.

### Conversion of Acrylic Fibrous Waste into AC Web

The acrylic fibers were separated from bath mats using

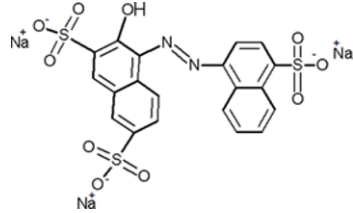
**Table 1.** Physical properties of acrylic fibers

Physical properties	
Tenacity (g/D)	0.3
Fineness (D)	9
Elongation (%)	50-52
Shrinkage (%)	2.5

mechanical cutting. The fibers were further opened on laboratory roller card (Befama, Poland) and converted into compact structure of non-woven web using needle punching machine. The speed of feeding the carded web to needle punching machine was fixed at the rate of 0.4 m/s. The frequency of strokes was maintained at 200 (Strokes per minute) with 5 mm depth of needle penetration. This produced the web having thickness of 11.6 mm and density 2.78 g/cm<sup>3</sup>. The schematic diagram for the formation of activated web is shown in Figure 1.

The acrylic fibrous web was then cut into 30 cm (length) and 30 cm (width) for subsequent high temperature treatment using high temperature furnace. The acrylic non-woven web was initially stabilized with 35 °C/h up to 250 °C to minimize

**Table 2.** Structure and properties of acid red 27

Acid red 27	
Chemical structure	
Molecular formula	C <sub>20</sub> H <sub>11</sub> N <sub>2</sub> Na <sub>3</sub> O <sub>10</sub> S <sub>3</sub>
Molecular weight	604.47
Color index number	16185

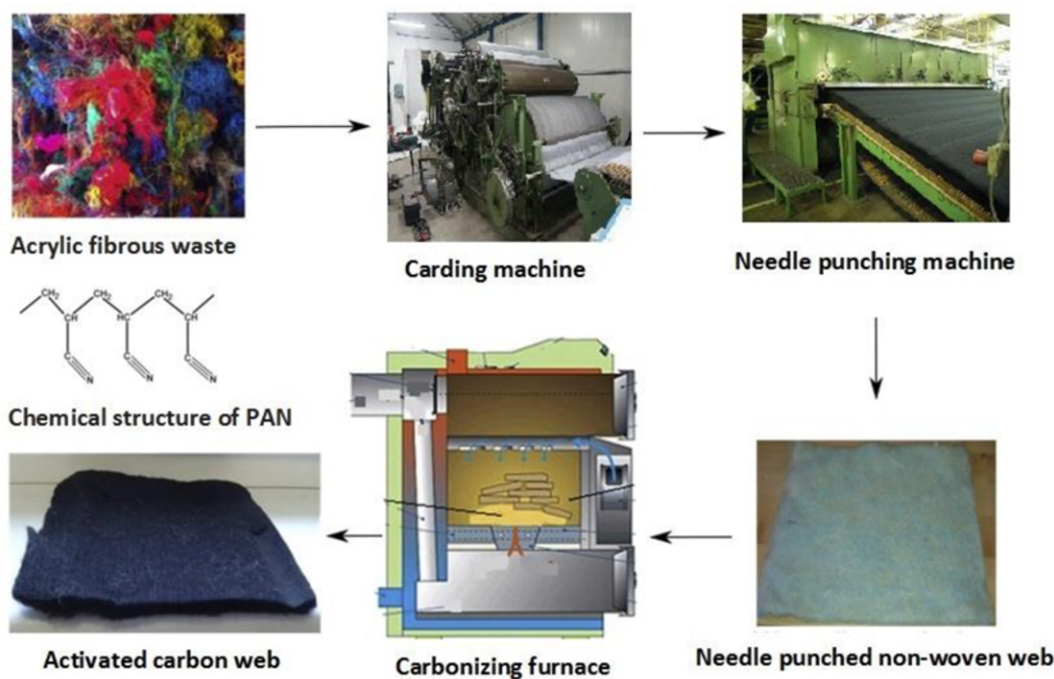


**Figure 1.** Schematic diagram of AC web from acrylic fibrous waste.

**Table 3.** Carbonization parameters for acrylic fibrous waste

Sample no.	Final pyrolysis temperature (°C)	Heating rate (°C/h)
1	800	150
2	800	300
3	800	450
4	1000	150
5	1000	300
6	1000	450
7	1200	150
8	1200	300
9	1200	450

the shrinkage during carbonization. During stabilization, predetermined tension was applied to avoid shrinkage. Later, the stabilized web was carbonized to 800 °C, 1000 °C, and 1200 °C with different heating rates (150, 300, and 450 °C/h) and no holding time (holding time means the length of time the web was placed at high temperature) under the layer of charcoal to find better values of yield and surface area as can be seen from Table 3.

#### Characterization of Prepared AC Web

The activated carbon webs prepared at different temperatures were characterized for determining their flexibility, yield, dusting, specific surface area, and elemental analysis. The yield of activated carbon web was determined from equation (1).

$$\text{Yield} = \frac{\text{Final weight of AC web}}{\text{Initial weight of acrylic web}} \times 100 \quad (1)$$

The flexibility of carbonized webs was determined by using cantilever bending principle (ASTM D 1388). The dusting behavior of activated carbon webs was determined by rubbing the webs after certain time (ASTM D 3884). The specific surface area of activated carbon webs was determined by nitrogen adsorption-desorption isotherms at 77.3 K using a Quantachrome instrument. The isotherms were taken in relative pressure  $P/P_0$  (range from 0.02 to 1). The samples were pre-treated in an oven at 45 °C in dry-room for at least 5 h, and then out gassed overnight at 300 °C prior to the adsorption analysis. Both adsorption and desorption isotherms were measured and the specific surface area was determined. Energy dispersive X-ray (EDX) analysis was done to find out the different elements and their concentrations. Fourier transform infrared spectroscopy (FTIR) analysis was carried out to confirm the functional groups present on the surface of acrylic fibrous wastes and prepared activated carbon. It was performed on a Nicolet iZ10, Thermo Scientific Inc, USA using reflection ATR technique on an adapter with a crystal of ZnSe in wavenumber

range of 600 to 4000  $\text{cm}^{-1}$ . The number of scans was 16 and a resolution was 4  $\text{cm}^{-1}$ . X-ray diffraction (XRD) is a technique used for the identification of crystalline material and analysis of unit cell dimensions. Degree of crystallinity can be calculated from equation (2).

$$I_c = 1 - \frac{I_1}{I_2} \quad (2)$$

where  $I_1$  is intensity at minimum peak and  $I_2$  is intensity at maximum peak.

#### Adsorption of Acid Red 27 on to AC Non-Woven Web

The aqueous solution of acid red with different concentrations was prepared by dissolving the required amount of dye in distilled water. For determining adsorption performance different concentrations (5.0, 10.0, 15.0, 20.0, and 25.0 mg/l) of Acid red 27 was used. The adsorption performance was investigated by using batch method. A constant amount of AC web (i.e. 0.1 g) was introduced in each flask having 50 ml of dye solution and was placed on a water bath shaker for 200 rpm to ensure that equilibrium was achieved. After set intervals of time, the dye solution was examined with the help of UV-visible spectrophotometer (UV-1600 pc spectrophotometer). The dye removal efficiency was calculated from equation (3).

$$\text{Dye removal efficiency} = \left[ \frac{(C_0 - C_e)}{C_0} \right] \times 100 \quad (3)$$

where  $C_0$  (mg/l) and  $C_e$  (mg/l) are initial and final concentrations of dye before and after the addition of adsorbent (activated carbon web), respectively. The adsorption capacity of activated carbon web was calculated from equation (4).

$$\text{Adsorption capacity } (q_e) = (C_0 - C_e) \frac{V}{W} \quad (4)$$

where  $q_e$  (mg/g) is the amount of dye adsorbed or accumulated on adsorbent,  $V$  is the volume of solution in liters, and  $W$  is the mass of adsorbent in grams.

#### Morphology of AC Web after Dye Adsorption

The morphology of activated carbon and dye adsorbed activated carbon web was studied by the help of a scanning electron microscope (SEM) at 30 kV accelerated voltage.

#### Adsorption Isotherms

The adsorption isotherms explain the distribution of adsorbate (dye molecules) in liquid phase and adsorbent, when the equilibrium is achieved [14]. Langmuir and Freundlich isotherms were used to explain the distribution of adsorbate molecules and their adsorption mechanism on activated carbon. The Langmuir believes in monolayer adsorption, while Freundlich endorses heterogeneity of adsorbent surface and multi-layer adsorption capacity [15].

### Langmuir Isotherm

The Langmuir isotherm is described by the equation (5).

$$q_e = \frac{q_{\max} K_L C_e}{1 + K_L C_e} \quad (5)$$

After linearization the Langmuir equation becomes as given in equation (6).

$$\frac{C_e}{q_e} = \frac{1}{q_{\max} K_L} + \frac{C_e}{q_{\max}} \quad (6)$$

where  $K_L$  is Langmuir constant for rate of adsorption (l/mg),  $q_{\max}$  is Langmuir constant for maximum dye adsorption capacity (mg/g),  $q_e$  is the amount of dye adsorbed per unit mass of adsorbent (mg/g), and  $C_e$  is the concentration of dye at equilibrium (mg/l).

### Freundlich Isotherm

The non-linear form of Freundlich isotherm is given by equation (7).

$$q_e = k_F C_e^{1/n} \quad (7)$$

The linear form of Freundlich equation is given by equation (8).

$$\log q_e = \ln k_F + \frac{1}{n} \ln C_e \quad (8)$$

where  $1/n$  is Freundlich constant for intensity of adsorption (l/mg) and  $k_F$  is Freundlich constant for adsorption capacity (mg/g).

### Kinetic Mechanisms

The adsorption mechanism on activated carbon was analyzed by using pseudo first order and pseudo second order model. The pseudo first order model is described by equation (9).

$$\frac{dq_t}{dt} = k_1(q_e - q_t) \quad (9)$$

where  $k_1$  is the equilibrium rate constant of adsorption ( $\text{min}^{-1}$ ),  $q_e$  and  $q_t$  are the amounts of dye adsorbed at equilibrium and at time  $t$  (min), respectively. After integrating above equation with boundary conditions from  $q_t=0$  to  $q_t=q_e$  and  $t=0$  to  $t$ , the above equation becomes

$$q_t = q_e(1 - e^{-k_1 t}) \quad (10)$$

The equation (9) after linearization becomes as shown in equation (11).

$$\log(q_e - q_t) = \log q_e - \frac{k_1 t}{2.303} \quad (11)$$

Pseudo second order kinetics is expressed as

$$\frac{dq_t}{dt} = k_2(q_e - q_t)^2 \quad (12)$$

After integrating the above equation becomes

$$q_t = \frac{k_2 q_e^2 t}{1 + k_2 t} \quad (13)$$

After linearization the above equation becomes equation (14).

$$\frac{t}{q_t} = \frac{1}{k_2 q_e^2} + \frac{t}{q_e} \quad (14)$$

## Results and Discussion

### Effect of Carbonization Parameters on the Properties of AC Web

The physical properties of activated carbon webs prepared at different temperatures (800 °C, 1000 °C, and 1200 °C) with different heating rates (150, 300, and 450 °C/h) and no holding time are shown in Table 4.

Initially the acrylic webs were stabilized at 250 °C with slow heating rate (35 °C/h). Black color after stabilization indicated that web was properly stabilized due to cyclization, dehydrogenation, and oxidation of PAN structure [16]. During stabilization, nitrile groups assisted in formation of ladder structure which enhanced mechanical properties and yield of final carbon web. During carbonization process, further crosslinking converted stabilized web into turbostratic carbon structure with more orientation of carbon basal planes. The activated carbon web prepared at 800 °C with heating rate 150, 300, and 450 °C/h provided surface area of 104, 120, and 90  $\text{m}^2/\text{g}$ . Similarly, at 1000 °C, it was 170, 190, and 140  $\text{m}^2/\text{g}$ , whereas at 1200 °C the achieved surface

**Table 4.** Effect of carbonization parameters on AC web properties

Temperature (°C)	Yield (%)	Flexibility	Dusting
Heating rate (150 °C/h)			
800	56.62	Good	Good
1000	49.32	Good	Good
1200	37	Poor	Poor
Heating rate (300 °C/h)			
800	61.70	Good	Good
1000	57.14	Average	Average
1200	45.33	Poor	Poor
Heating rate (450 °C/h)			
800	63.47	Good	Good
1000	61.38	Poor	Poor
1200	51.56	Poor	Poor

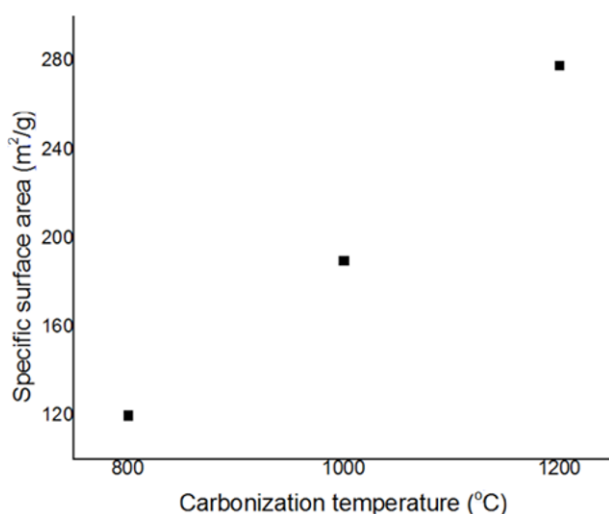


**Figure 2.** Effect of carbonization temperature on specific surface area of AC web.

area were 240, 278, and 210 m<sup>2</sup>/g at heating rate of 150, 300, and 450 °C/h, respectively (Figure 2).

The increase in surface area at high temperature was due to more reaction of atmospheric oxygen with carbonizing structure, which caused elimination of different elements from structure and rearrangement of basal planes. These two reasons were main driving forces for creation of porous structure. With increase of temperature, more reactions of carbonizing material caused more elimination of volatile gases and tarry matter resulted in higher carbon content despite of a decrease in the yield of carbon. At high heating rate, sudden rise of temperature caused fusion of carbonized structure due to which surface area was reduced and poor behavior of flexibility and dusting can be seen. However, the reduction of surface area at slow heating rate was due to prolonged carbonization which caused more oxidation of carbon and resulted in lesser yield. From the results obtained, the heating rate of 300 °C/h was found more appropriate for getting larger surface area along with appropriate yield. Figure 2 showed the increase of surface area with rise of temperature from 800 to 1200 °C at heating rate of 300 °C/h.

Figure 3 shows the nitrogen adsorption-desorption isotherm of activated carbon prepared at the carbonization temperature of 1200 °C, the heating rate of 300 °C/h without holding time. A rapid rise in the adsorption-desorption isotherm was found at low relative pressures, which was followed by a horizontal plateau at higher relative pressures. This behavior indicated type I isotherm based on the classification of the International Union of Pure and Applied Chemistry (IUPAC). The type I isotherm confirmed that micropore was developed in the prepared activated carbon. The pore volume and pore diameter of prepared activated carbon were found 0.437 cc/g and 3.062 nm, respectively from BJH analysis. In accordance to IUPAC classification, the adsorbent pores are classified

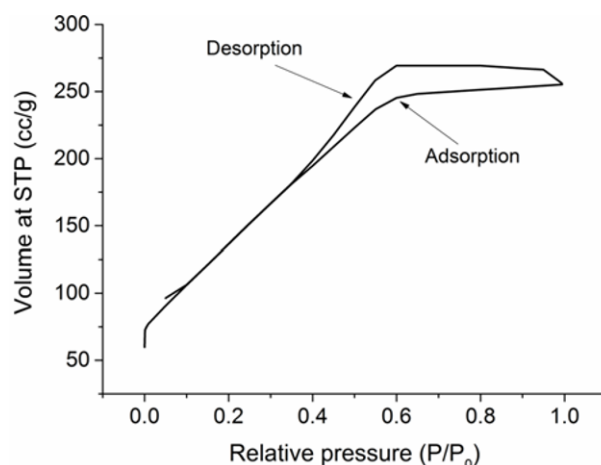


**Figure 3.** Nitrogen adsorption-desorption isotherm of activated carbon.

into three groups: micropore (diameter < 2 nm), mesopore (2-50 nm), and macropore (>50 nm). Therefore, the prepared activated carbon predominantly exhibited the micro and mesoporous nature.

#### Energy Disperse X-ray Spectroscopy Analysis

Energy disperse X-ray spectroscopy analysis (EDX) gave the relative proportion of different elements present in carbon webs prepared at different temperatures (800, 1000, and 1200 °C) with the heating rate of 300 °C/h as can be seen from Table 5.

It was clear from Table 5 that by increasing the carbonization temperature from 800 °C to 1200 °C the carbon content was increased, however, with reduction in concentration of oxygen. The AC web produced at 1200 °C showed 92.49 % and 6.61 % content of carbon and oxygen, respectively due to the elimination of nitrogen, sulfur, hydrogen, and other elements [17,18].

**Table 5.** Effect of carbonization temperature on elemental composition of AC web

Element	App conc.	Intensity	Weight (%)	Atomic (%)
800 °C				
CK	0.26	2.12	0.13	91.76
OK	0.01	0.761	0.01	8.24
1000 °C				
CK	0.37	2.12	0.18	91.87
OK	0.02	0.760	0.02	8.13
1200 °C				
CK	0.18	2.10	0.09	92.49
OK	0.01	0.744	0.01	6.61
CaK	0.00	0.902	0.00	0.90

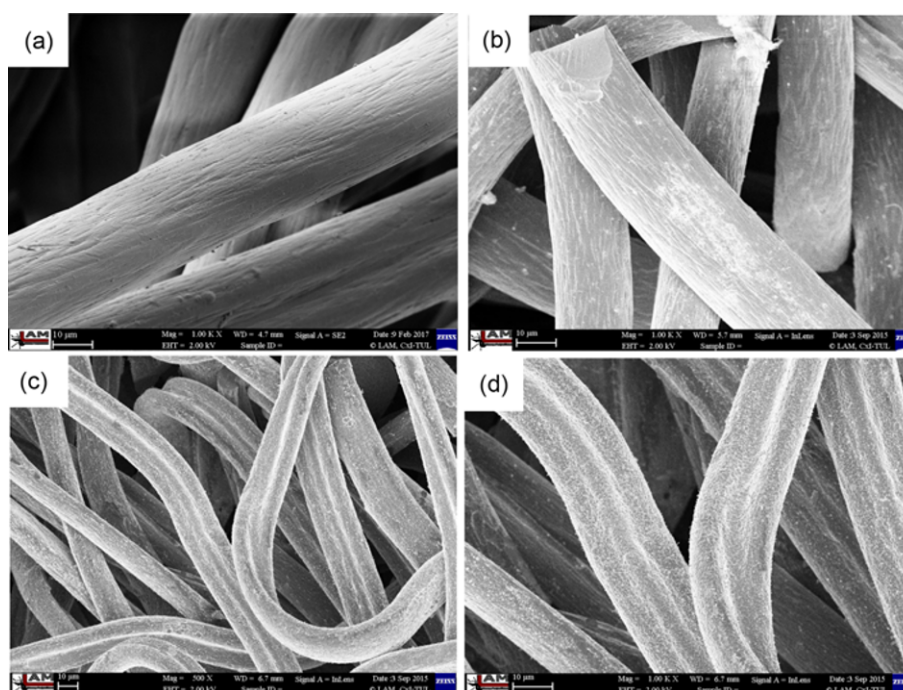


**Figure 4.** SEM images; (a) acrylic web, (b) AC prepared at 800 °C, (c) AC prepared at 1000 °C, (d) SEM image of AC prepared at 1200 °C.

### SEM Morphology

For determination of porosity, the surface morphology of activated carbon webs prepared at different temperatures was analyzed. Figure 4(a)-(d) showed the SEM images of pure acrylic and AC webs produced at 800 °C, 1000 °C, and 1200 °C. It was clear from SEM images that as temperature of carbonization increased, roughness of surfaces also increased. The increased surface roughness indicated the more porous structure at high temperature.

The functional groups present on the surface of activated carbon highly influence its adsorption characteristics as well as its adsorption capabilities. Fourier transform infrared spectroscopy was carried out to confirm the presence of different functional groups (i.e. hydroxyl, carboxyl, methyl, or aromatic rings) on the surface of activated carbon. Figure 5 shows these spectra for acrylic fibrous waste and prepared activated carbon sample after physical activation in presence of air. When comparing the two spectra between acrylic fibrous waste and prepared activated carbon, the disappearance of many absorption bands were found in case of prepared activated carbon spectrum due to the action of carbonization and activation. This suggested the decomposition and subsequent release of by-products as volatile matter by physical activation of acrylic fibrous waste at high temperature. The peaks at the range of 1500-1000  $\text{cm}^{-1}$  correspond to carbonyl group, carboxylate ion, ash component, and chelate bonded carboxylate structures on prepared activated carbon, whereas the small peaks at 2939.5 and 2862.6  $\text{cm}^{-1}$  represent the C-H stretching vibration in methyl group.

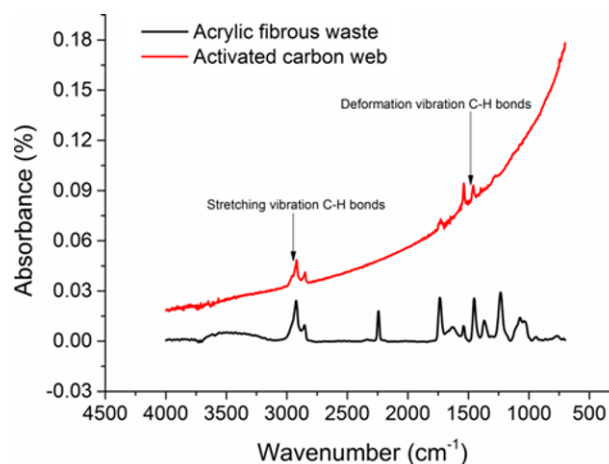


**Figure 5.** FTIR spectra of acrylic fibrous waste and activated carbon.

### Effect of Process Parameters on Dye Removal Efficiency Effect of Initial Concentration of Dye

The dye adsorption performance of activated carbon was investigated by varying the initial concentration of dye from 5 mg/l to 25 mg/l. It is clear that dye removal percentage increased by increasing contact time and then achieved a constant value when the process reached at equilibrium as can be seen from Figure 6(a). At low concentration of dye, the equilibrium process was achieved earlier because of more available active sites for adsorption of dye molecules [15]. As far as dye removal efficiency was concerned, it

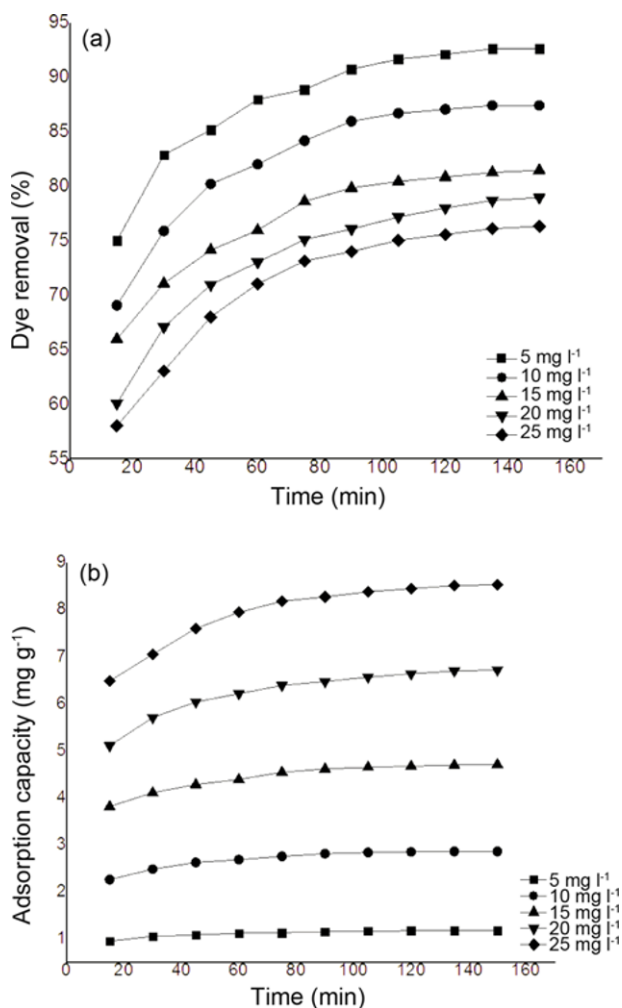


**Figure 6.** (a) Effect of dye concentration on dye removal efficiency and (b) effect of initial concentration of dye on adsorption capacity of activated carbon.

decreased from 92.59 % to 76.31 % when the concentration of dye was increased from 5 mg/l to 25 mg/l while keeping other factors constant like dosage of activated carbon, stirring speed, and temperature. Similarly, when the dye concentration was increased from 5 mg/l to 25 mg/l, the dye accumulated on activated carbon was also found to increase from 0.95 mg/g to 6.48 mg/g as can be seen from Figure 6(b). However, with the increase of contact time at a particular dye concentration, the adsorption capacity was reduced. The adsorption capacity decreased as it was related to the capacity of adsorbent material which decreased by accumulation of dye molecules on the activated carbon.

**Effect of Adsorbent Dosage**

The effect of adsorbent dosage on dye removal efficiency and adsorption capacity was analyzed by changing the adsorbent dosage from 1 mg/l to 5 mg/l while keeping other factors same like contact time 150 min, temperature 25 °C,

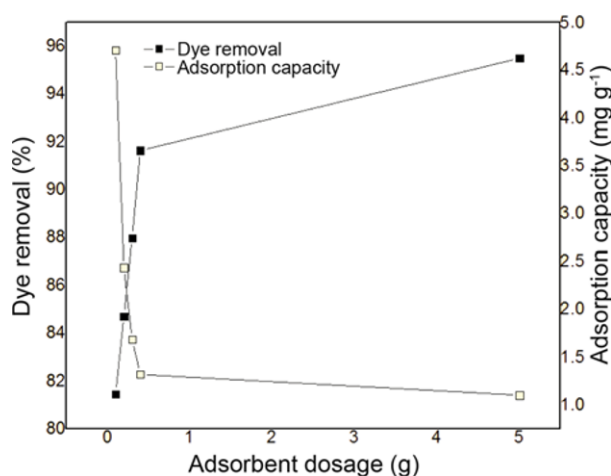


**Figure 7.** Effect of adsorbent dosage on dye removal and adsorption capacity.

15 mg/l acid red concentration, and a stirring speed of 200 rpm. From Figure 7, it is clear that dye removal efficiency increased as the quantity of activated carbon was increased. The acid red removal percentage was 81.46 % when 1 g/l adsorbent (activated carbon) was used. However, this trend of dye removal efficiency kept on increasing to 84.72 %, 87.98 %, 91.64 %, and 95.51 % when the quantity of activated carbon was increased to 2 g/l, 3 g/l, 4 g/l, and 5 g/l, respectively. This increase in dye removal efficiency is attributed to increased surface area of adsorbent and more availability of active sites resulting from increased adsorbent dosage. Similar results have been reported by removal of acid dye on granular AC [19,20]. However, there was an inverse trend when the adsorbent dosage and adsorption capacity of activated carbon were analyzed. This is probably due to the reason that adsorption sites present on activated carbon remained unsaturated in adsorption process, hence a fall in adsorption capacity was expected [21,22].

**Effect of Stirring Speed**

The effect of stirring speed on dye removal efficiency and adsorption capacity was investigated by keeping acid red concentration 6 mg/l, temperature 25 °C, adsorbent dosage 2 g/l, and contact time 150 min to ensure that equilibrium point was achieved. The stirring speed was changed from 50 rpm to 200 rpm. One sample was used without the stirring speed for comparing the results. From Figure 8, it is clear that only 2.44 % dye was removed without any stirring. However, as the stirring speed was increased, dye removal efficiency was found to increase to 30.75 %, 57.23 %, 71.89 %, and 81.78 %, respectively. As far as adsorption capacity was concerned, it also increased with the stirring speed. The adsorption capacity of activated carbon increased from 1.78 mg/g to 3.31 mg/g, 4.155 mg/g, and 4.71 mg/g when the stirring speed was increased from 50 rpm to 100 rpm, 150 rpm, and 200 rpm, respectively. This trend is obvious due to more interaction of dye solution with the adsorbent at

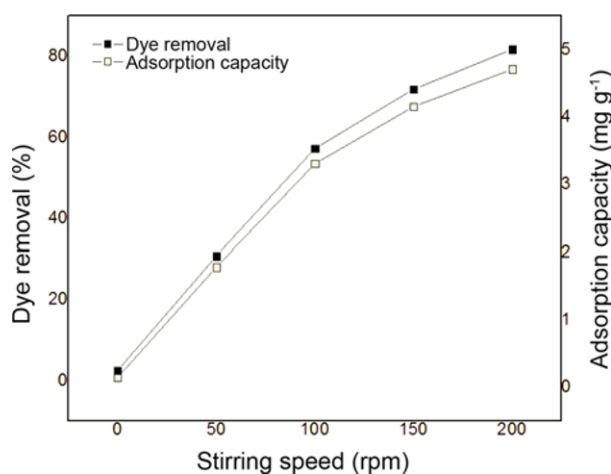


**Figure 8.** Effect of stirring speed on dye removal and adsorption capacity.

high stirring speed [22].

#### Effect of pH

The pH of solution has significant effect on the dye removal efficiency and adsorption performance of activated carbon. For analyzing dye removal efficiency of acid red, pH of solution was varied from 2 to 11, while keeping other parameters constant like adsorbent dosage 2 mg/l, dye concentration 15 mg/l, stirring speed of 200 rpm, temperature 25 °C, and contact time 150 min to ensure that equilibrium was achieved. The point of zero charge of AC web prepared by pyrolysis of acrylic fibrous waste was found to be 5.90. It is the point at which the net charge on the surface of activated carbon is zero [23]. At  $\text{pH} > \text{pH}_{\text{ZPC}}$  the surface of adsorbent is negatively charged while at  $\text{pH} < \text{pH}_{\text{ZPC}}$  the surface becomes positively charged [24,25]. The pH of solution was varied by the help of sodium hydroxide (NaOH) and hydrochloric acid (HCL). It is clear from Figure 9 that maximum dye removal efficiency (93.27 %) was observed at pH 2, while minimum dye removal (67.82 %) was observed at pH 11. At pH value lower than the point of zero charge of activated carbon, the surface of activated carbon becomes positively charged due to accumulation of positive ions ( $\text{H}^+$ ). Therefore, as the pH value was reduced, the adsorption capacity and dye removal efficiency was increased due to electrostatic attraction between positively charged activated carbon and anionic dye molecules (AR<sup>-</sup>). This force of attraction is mainly responsible for the removal of dye molecules from the solution. However, as the pH of solution was increased further, the dye removal efficiency and adsorption capacity decreased due to accumulation of negatively charge on the surface of adsorbent. This force of repulsion between anionic dye molecules and surface of activated carbon was mainly responsible for less removal of dye at high pH. Similar results have been reported by Shah and coworkers [26] where they found that electrostatic force of attraction and repulsion had significant effect on dye

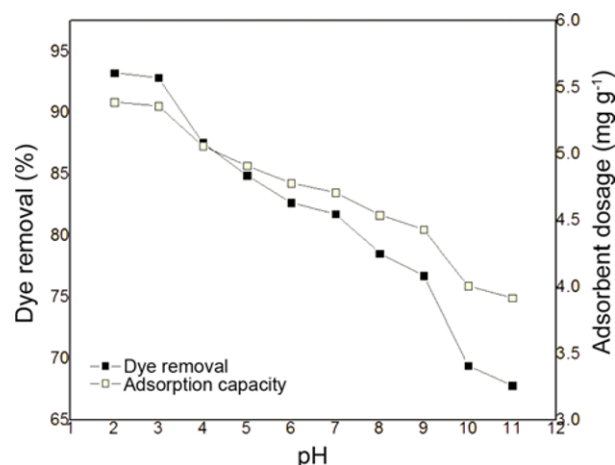


**Figure 9.** Effect of pH on dye removal efficiency and adsorption capacity.

removal from solution.

### Adsorption Isotherms

#### Langmuir Isotherm

Langmuir model believes in monolayer adsorption of adsorbate (dye molecules) because of uniform energies of adsorption sites [27]. For determining Langmuir isotherm, the non-linear plot of  $C_e$  versus  $q_e$  for adsorption of acid red onto activated carbon derived from acrylic fibrous waste at 25 °C are shown in Figure 10. The intercept and slope from the non-linear plot of  $C_e$  versus  $q_e$  were used to estimate  $K_L$  and  $q_{\text{max}}$  in Table 6 along with their standard errors. The value of  $R^2$  (coefficient of determination) from Langmuir isotherm was found to be .995 with SSE (0.005). The value of  $R_L$  was calculated from the following equation.

$$R_L = \frac{1}{1 + K_L C_0}$$

where  $R_L$  is dimensionless equilibrium parameter which gives the information about the shape of isotherm as  $R_L = 0$  (irreversible),  $R_L = 1$  (linear),  $0 < R_L < 1$  (favorable), and  $R_L > 1$

**Table 6.** Parameters for adsorption isotherms

Langmuir adsorption isotherm	
$q_{\text{max}}$ (mg/g)	21.68±2.12
$K_L$ (l/mg)	0.067±0.009
$R_L$	0.49
$R^2$	0.995
SSE	0.057
Freundlich adsorption isotherm	
$K_F$	0.50±0.02
$1/n$	1.35±0.012
$R^2$	0.999
SSE	0.017



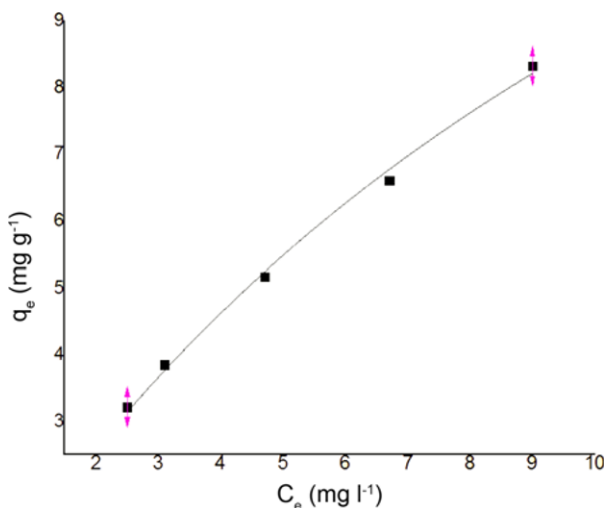


Figure 10. Non-linear form of Langmuir adsorption isotherm.

(unfavorable). The value of  $R_L$  calculated to be 0.49 which showed favorable adsorption of acid red on activated carbon.

**Freundlich Isotherm**

The Freundlich isotherm for the adsorption of acid red on activated carbon is shown in Figure 11 by plotting  $C_e$  versus  $q_e$ . From the respective plot of  $C_e$  versus  $q_e$ , the values of slope and intercept were found out which were used to calculate  $1/n$  and  $K_F$  as given in Table 6. The value of SSE is more in Langmuir isotherm than Freundlich isotherm which showed closer fit of results in Freundlich isotherm. This showed heterogeneous surface nature of activated carbon with non-homogenous presence of active groups. However, the value of  $1/n$  obtained is 1.35. The value of  $1/n$  is a function that gives the strength of adsorbent material. When the value of  $1/n$  is more than 1, it shows the adsorption coefficient increases by increasing the concentration of

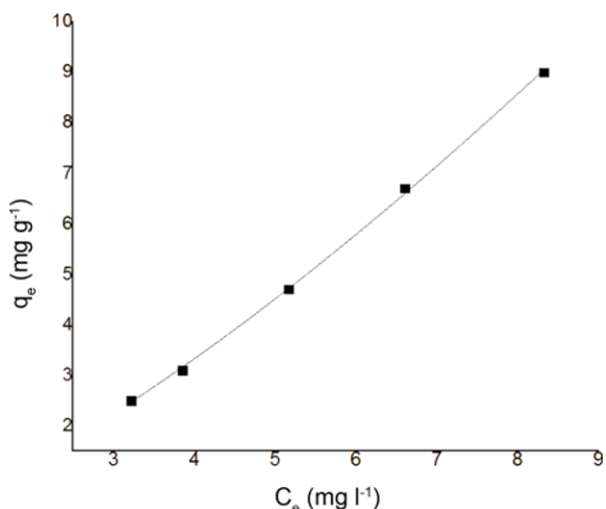


Figure 11. Non-linear form of Freundlich adsorption isotherm.

solution which led to increase in hydrophilic surface characteristic after mono layer adsorption [28]. Therefore, both Freundlich and Langmuir models could be used for the utility of present study.

**Adsorption Kinetics**

The adsorption kinetics is important in determining the adsorbate uptake by adsorbent and time required for the completion of process of adsorption [29]. The adsorption kinetics for acid red onto activated carbon was studied by using experimental data for linear and non-linear forms of pseudo first and second order models. The linear and non-linear forms of pseudo first order model were plotted by taking  $\log(q_e - q_t)$  on y-axis and time on x-axis, respectively, as can be seen from Figures 12 and 13. Similarly, the linear and non-linear forms of pseudo second order model were plotted by taking  $t/q_t$  on y-axis and time on x-axis and for non-linear  $q_e$  (y-axis) was plotted against time (x-axis), respectively, as shown in Figures 14 and 15.

From the intercept and slope of linear forms of pseudo

Table 7. Parameters of pseudo first order of acid red on AC

Kinetic model parameters	Initial concentrations (mg/l)				
	5	10	15	20	25
$q_{e,exp}$ (mg/g)	1.17	2.85	4.70	6.71	8.52
Linear model					
$q_{e,cal}$ (mg/g)	0.005	0.085	0.35	0.43	0.61
$K_1$	-0.0008	-0.0045	-0.0166	-0.0167	-0.0059
$R^2$	85.50	93.50	94.71	86.46	96.28
Non-linear model					
$q_{e,cal}$ (mg/g)	1.14	2.77	4.55	6.46	8.22
$K_1$	0.110	.100	0.109	0.092	0.088
$R^2$	74.96	74.30	65.43	75.80	71.83

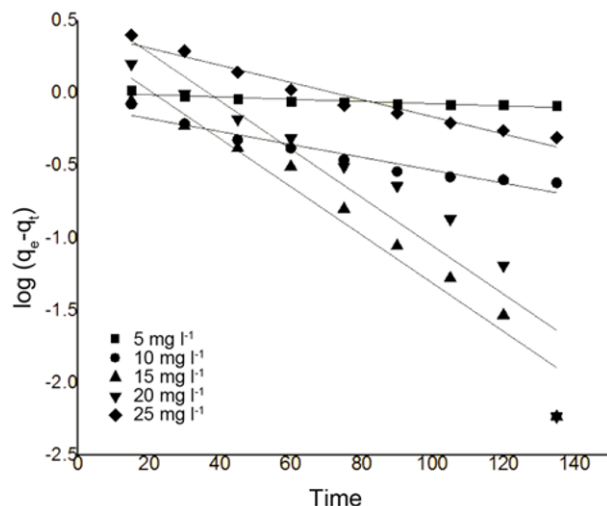


Figure 12. Linear form of Pseudo 1st order model.

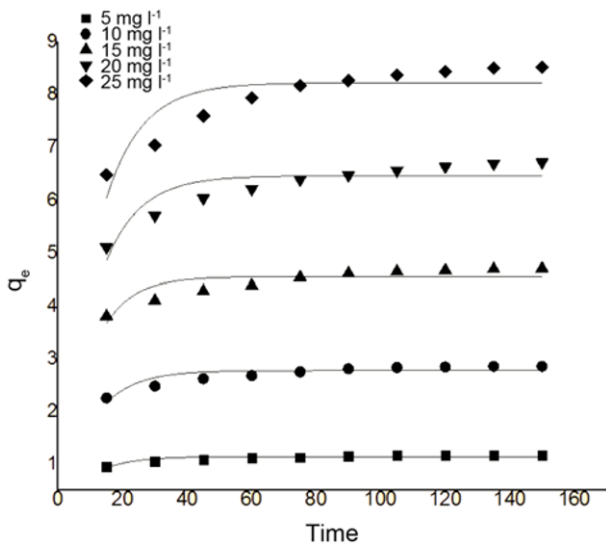


Figure 13. Non-linear form of pseudo 1st order model.

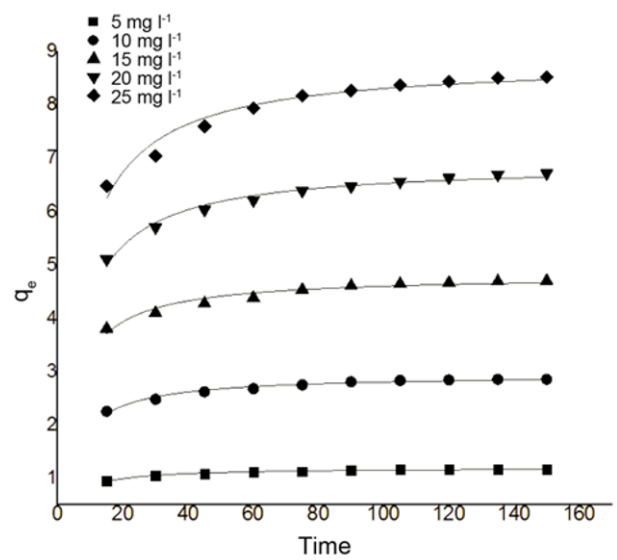


Figure 15. Non-linear form of pseudo 2nd order model.

Table 8. Parameters of pseudo second order of acid red on AC

Kinetic model parameters	Initial concentrations (mg l <sup>-1</sup> )				
	5	10	15	20	25
$q_{e,exp}$ (mg/g)	1.176	2.858	4.705	6.717	8.529
Linear model					
$q_{e,cal}$ (mg/g)	4.04	1.94	1.12	0.98	0.80
$K_1$	0.822	0.335	0.20	0.142	0.118
$R^2$					
Non-linear model					
$q_{e,cal}$ (mg/g)	1.20	2.94	4.80	6.90	8.82
$K_1$	0.198	0.068	0.047	0.025	0.018
$R^2$	97.78	97.40	94.43	97.65	95.61

first and second order model, the respective values of adsorption capacity ( $q_e$ ) and rate constants ( $k_1$  and  $k_2$ ) were calculated. Tables 7 and 8 give values of dye uptake and rate constants at different concentrations of dye. In linear form although correlation coefficient of pseudo second order was more appropriate, but the values predicted by both the models were far away from actual results and did not follow any trend. For getting values more close to practical results, the non-linear curve fitting by using origin pro was used. In non-linear curve fitting, both models predicted values very much close to practical values. However, the higher values of  $R^2$  for pseudo second order model suggested this model to be more effectively employed for the adsorption behavior of acid red on activated carbon.

### Conclusion

The acrylic fibrous waste was successfully converted into activated carbon web by physical activation at different temperatures (800 °C, 1000 °C, and 1200 °C) with different heating rates of 150, 300, and 450 °C/h with no holding time under the layer of charcoal. The higher surface area 278 m<sup>2</sup>/g was achieved at higher temperature 1200 °C with 300 °C/h due to more elimination of different elements from carbonized material and due to mutual arrangement of carbon sheets. Later, the adsorption performance of acid red on activated carbon was examined by varying different parameters like varying the initial concentration of dye from 5 mg/l to 25 mg/l, adsorbent dosage, stirring speed, and different pH of solutions. From the results, it is clear that more equilibrium time was required when the concentration of dye was increased. However, when the adsorbent dosage and stirring speed were increased, it took less time to remove dye. When

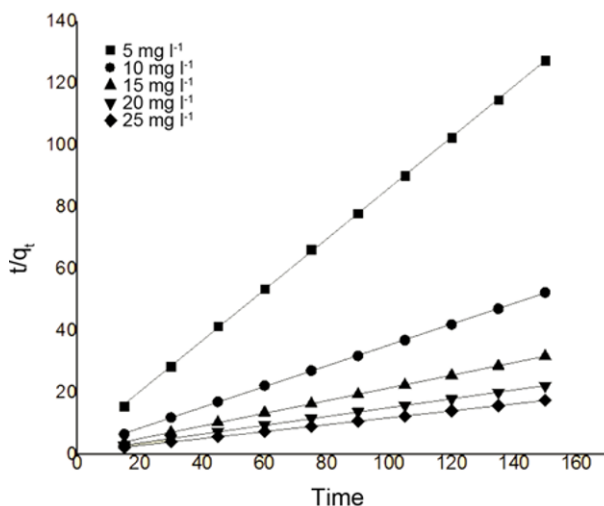


Figure 14. Linear form of Pseudo 2nd order model.

the experimental results were analyzed using non-linear forms of adsorption isotherms (Langmuir and Freundlich isotherms), the Freundlich isotherm showed more better fitting of results due to heterogeneous surface nature of activated carbon.

### Acknowledgement

This work was supported under the student grant scheme (SGS-21198) by Technical University of Liberec, Czech Republic.

### References

- V. K. Gupta and Suhas, *J. Environ. Manag.*, **90**, 2313 (2009).
- C. H. Huang, K. P. Chang, H. D. Ou, Y. C. Chiang, and C. F. Wang, *Microporous Mesoporous Mater.*, **141**, 102 (2011).
- E. Forgacs, T. Cserháti, and G. Oros, *Env. Int.*, **30**, 953 (2004).
- G. Ciardelli and N. Ranieri, *Water Res.*, **35**, 567 (2001).
- R. C. Bansal, "Activated Carbon Adsorption", 1st ed., pp.25-28, Taylor and Francis Group, London, 2005.
- F. S. Hashem and M. S. Amin, *J. Therm. Anal. Calorim.*, **116**, 835 (2014).
- S. M. A. El-Gamal, M. S. Amin, and M. A. Ahmed, *J. Env. Chem. Eng.*, **3**, 1702 (2015).
- F. S. Hashem, M. S. Amin, and S. M. A. El-Gamal, *Appl. Clay Sci.*, **115**, 189 (2015).
- M. A. Daley, C. L. Mangun, J. A. DeBarrb, S. Riha, A. A. Lizzio, G. L. Donnals, and J. Economy, *Carbon N. Y.*, **35**, 411 (1997).
- C. L. Mangun, M. A. Daley, R. D. Braatz, and J. Economy, *Carbon N. Y.*, **36**, 123 (1998).
- G. T. Sivy and M. M. Coleman, *Carbon N. Y.*, **19**, 137 (1981).
- M. A. Nahil and P. T. Williams, *J. Anal. Appl. Pyrolysis*, **89**, 51 (2010).
- V. Baheti, S. Naeem, J. Militky, M. Okrasa, and B. Tomkova, *Fiber. Polym.*, **16**, 2193 (2015).
- U. Gecgel, G. Ozcan, and G. C. Gurpinar, *J. Chem.*, **201**, 1 (2013).
- Z. Z. Chowdhury, S. M. Zain, R. A. Khan, and K. Khalid, *Orient. J. Chem.*, **27**, 405 (2011).
- Y. Liu, Y. H. Choi, H. G. Chae, P. Gulgunje, and S. Kumar, *Polym. Guildf*, **54**, 4003 (2013).
- M. A. Zaini, Y. Amano, and M. Machidaa, *J. Hazard. Mater.*, **180**, 552 (2010).
- S. Jagannathan, H. G. Chae, R. Jain, and S. Kumar, *J. Power Sources*, **185**, 676 (2008).
- S. Naeem, V. Baheti, V. Tunakova, J. Militky, K. Daniel, and B. Tomkova, *Carbon N. Y.*, **111**, 439 (2017).
- Y. Ma, X. Yin, and Q. Li, *Nonferrous Met. Soc.*, **23**, 1652 (2013).
- S. Marius, C. Benoit, C. Igor, D. Mariana, and P. Stelian, *Sci. Study Res.*, **12**, 307 (2011).
- I. Dahil, *Environ. J.*, **2**, 35 (2016).
- D. C. Sharma and C. F. Forster, *Water Res.*, **27**, 1201 (1993).
- S. Naeem, V. Baheti, J. Militky, J. Wiener, P. Behera, and A. Ashraf, *Fiber. Polym.*, **17**, 1245 (2016).
- M. A. Rahman, S. M. R. Amin, and A. M. S. Alam, *Dhaka Univ. J. Sci.*, **60**, 185 (2012).
- Y. Al-Degs, M. I. El-Barghouthi, A. El-Sheikh, and G. M. Walker, *Dye Pigment.*, **77**, 16 (2008).
- Y. Al-Degs, M. Khraisheh, S. Allen, and M. Ahmad, *Water Res.*, **34**, 927 (2000).
- I. Shah, R. Adnan, W. Ngah, and Y. Taufiq, *PLoS One*, **10** (2015).
- R. Baccar, P. Blázquez, J. Bouzid, M. Feki, and M. Sarrà, *Chem. Eng. J.*, **165**, 457 (2010).
- M. Ismail, C. N. Weng, H. Abdul Rahman, and A. Zakaria, *J. Geogr. Earth Sci.*, **1**, 1 (2013).
- A. Demirbas, *Energy Sources Part A*, **31**, 217 (2009).